Chinese Journal of Polymer Science Vol. 35, No. 6, (2017), 764−772

Chinese Journal of Polymer Science

Effects of Ultra-high Temperature Treatment on the Microstructure of Carbon Fibers*

Wei-wei Li[a, b], Hong-liang Kang[a], Jian Xu[a**] and Rui-gang Liu[a**]

[a] *Laboratory of Polymer Physics and Chemistry, Beijing National Laboratory for Molecular Science, Institute of Chemistry, Chinese Academy of Sciences, Beijing 100190, China*

[b] *University of Chinese Academy of Sciences, Beijing 100049, China*

Abstract The microcrystalline structure and microvoid structure in carbon fibers during graphitization process (2300−2700 °C) were characterized employing laser micro-Raman scattering (Raman), X-ray diffraction (XRD), small angle X-ray scattering (SAXS), and high-resolution transmission electron microscopy (HR-TEM). The crystalline sizes (L_a, L_c) increased and interlayer spacing (d_{002}) decreased with increasing heat treatment temperature (HTT). The microvoids in the fibers grew up and contacted to the neighbors with the development of microcrystalline. In addition, the preferred orientation of graphite crystallite along fiber axis decreased and microvoids increased. The results are crucial for analyzing the evolution of microstructure of carbon fibers in the process of heat treatment and important for the preparation of high strength and high modulus carbon fibers.

Keywords Carbon fibers; Graphitization; Microcrystalline structure; Microvoid structure

INTRODUCTION

Carbon fibers have many unique properties, such as high strength, high modulus, low density, low expansion, corrosion resistance and thermostability. These unique characteristics offer excellent properties to the carbon fiber reinforced composites that have versatile applications in the fields of aircraft industry, medical instruments, transportation, sports facilities, new energy exploitation and so on. There are three main steps in preparation of carbon fibers from precursor including pre-oxidization or stabilization, carbonization and graphitization[1]. Graphitization is a process of crystallization of graphite sheets in carbon fibers, as well as a process to refine the crystal structure. The graphitizing process is critical in the preparation of high modulus carbon fibers, during which the amorphous and disordered carbon structure rearrange into well-ordered three dimensional graphite structure at high treatment temperature.

The mesophase pitch is the best candidate for preparing high-modulus carbon fibers if modulus alone is the only requirement, owing to the preferred orientation of the layer planes. While polyacrylonitrile (PAN)-based carbon fibers have a complex structure of interlinked layer planes, their tensile strength is higher than that of mesophase pitch based carbon fibers. Therefore, PAN-based carbon fibers become the best choice of carbon fibers with excellent combination properties. The PAN-based carbon fibers account for 90% market of carbon fibers worldwide due to its high quality. With the proper high temperature graphitization treatment, PAN-based

* This work was financially supported by the National High Technology Research and Development Program of China (863 Program, No. 2015AA03A204).

** Corresponding authors: Jian Xu (徐坚), E-mail: jxu@iccas.ac.cn
Rui-gang Liu (刘瑞刚), E-mail: rgliu@iccas.ac.cn

Received September 18, 2016; Revised November 30, 2016; Accepted December 2, 2016
doi: 10.1007/s10118-017-1922-9

carbon fibers with high strength and high modulus can be produced.

The mechanical properties of carbon fibers are directly related to the microstructures of three dimensional graphitic microcrystals, including the size, stacking states and orientation of the graphite structure in the carbon fibers[2–4]. The investigation of the relationship between microstructure of carbon fibers and process parameters is important for controlling the structure, properties, and quality of carbon fibers.

There are several methods to characterize the microcrystalline structure of carbon fibers. The most popular methods to determine microcrystalline structure of carbon materials are Raman spectroscopy[5–7], X-ray diffraction (XRD)[5, 8], and transmission electron microscopy (TEM)[4, 9]. With the development of the technology of small angle X-ray scattering (SAXS)[10, 11], theory and method using SAXS for the characterization of the microvoids in carbon fibers have also been established and developed in the last twenty years[10, 12–15]. The microvoids in carbon fibers either form or pass down from the microvoids in the precursors during the stabilization, carbonization and graphitization processes. Microvoids are a kind of defects in the carbon fibers and therefore it is better to avoid or reduce their existence during the processing procedures of carbon fibers.

In this work, high temperature treatment of carbon fibers in the range of 2300–2700 °C was carried out on a continuous industrial graphitization line. The microcrystalline structure and microvoids in carbon fibers were investigated by using Raman spectroscopy, XRD, HR-TEM and SXAS. The effects of the treatments on the microstructure of the carbon fibers will be discussed. This work provides valuable information for high strength and high modulus PAN-based carbon fibers.

EXPERIMENTAL

Materials

PAN-based carbon fibers (Toray T700s, 6K) were used. Graphitization of the carbon fibers was performed on a continuous graphitization producing line at Gansu Haoshi Carbon Fiber Co., Ltd. China. The carbon fibers were treated at the temperatures of 2300–2400 °C, 2400–2500 °C, 2500–2600 °C, and 2600–2700 °C in a high purity argon atmosphere. The feeding speed and take-up speed were kept equal during the graphitization, that is, the length of the carbon fibers was kept at constant during the graphitization.

Characterization

Raman spectroscopy

The Raman measurements were performed on a Thermo Scientific DXR Raman microscope equipped with a 532 nm argon-ion laser line as the excitation source in the range of 500–3000 cm^{-1}. The characteristic peak at about 1580 cm^{-1} resulted from the stretching vibration of C—C, corresponding to the vibration mode of E_{2g2} in graphite lattice[6, 16], and marked as G-line. The peak width and position of the disorder-induced line at 1360 cm^{-1} were highly sensitive to defect of graphite lattice, disarranged and low-symmetrical carbon structure, corresponding to the vibration mode of A_{1g} in graphite lattice, and marked as D-line. There was another peak, located at 1620 cm^{-1}, marked as D′-line, which partially merged with the G-line. The D- and D′-lines are usually Raman-inactive, which became active due to phonon confinement caused by the defects. The degree of graphitization (R) was calculated by $R = I_D/I_G$. In order to improve the determination accuracy of the spectroscopic parameters, such as peak position, intensity, width, and shape, a Lorentz multiple peaks fitting procedure was employed.

X-ray diffraction (XRD)

XRD measurements were performed on a PANalytical X′Pert Pro MPD $\theta/2\theta$ X-ray diffractometer using nickel filtered Cu Kα radiation (λ = 0.154 nm). Bundles of carbon fibers of about 12000 filaments were aligned in parallel with a width of 5 mm and fixed on a matched die. The interlayer space/distance (d_{002}) and the average layer thickness (L_c) of (002) layer plane were calculated from the XRD traces obtained along the equator of the carbon fibers. The parameter of apparent crystallite length (L_a) was calculated from the XRD traces of along the meridianal direction in (100) plane. The preferred orientation angle (Z) of graphite crystallites along fiber axis

was obtained by azimuthal scanning in crystal face (002).

The interlayer spacing d_{002} was estimated according to Bragg equation (Eq. 1)[8, 17]. Crystal size parameters L_c and L_a were calculated by Scherrer's formula (Eq. 2). The orientation angle (Z) was calculated by using Eq. (3).

$$d_{002} = \frac{\lambda}{2\sin\theta} \tag{1}$$

$$L = \frac{K\lambda}{\beta\cos\theta} \tag{2}$$

$$Z = \frac{\text{FWHM}}{2} \tag{3}$$

where θ is the Bragg angle of corresponding reflection peak. λ is the wavelength of X-ray. The constant K is assigned as 0.89 and 1.84 for (002) and (100), respectively. β is the full width at half maximum intensity (FWHM) of the (002) at $2\theta \approx 25°$ and (100) at around $2\theta \approx 43°$. $\beta = (B^2 - b^2)^{1/2}$, in which B is apparent FWHM, and b is a broaden constant caused from diffractometer. FWHM is half of the diffraction intensity distribution of the azimuth scanning of (002). β and FWHM were obtained using a Gaussian-Lorentzian curve fitting procedure.

High resolution transmission electron microscopy (HR-TEM)

HR-TEM lattice fringe images of carbon fibers were observed on JEOL JSM-2200FS TEM with an acceleration voltage of 200 kV. The carbon fiber samples coated with epoxy resin at room temperature were then solidified at 75 °C for 12 h in a vacuum oven. Ultrathin slices for TEM observation were cut from the samples perpendicular to the axis of the carbon fibers using a Leica Ultra Cut R Ultra Microtome and fixed on copper grids.

Small angle X-ray scattering (SAXS)

SAXS experiments were carried out at the beam line BL16B1 SAXS system at Shanghai Synchrotron Radiation Facility (SSRF), China. The energy of X-ray was 10 keV and wavelength was 0.124 nm. The distance from the detector, a Marresearch Mar165 CCD, to samples was set at 5060 mm. The carbon fibers were arranged as aligned multifilament bundles fixed parallel on a matched metal frame with a window for X-ray irradiation. Each sample was exposed to X-rays for 1 s. The primary data were evaluated using the software package FIT2D. The beam center was corrected and the absorption by air was subtracted.

The parameters of voids in carbon fibers were calculated according to the method described in the literatures[10, 11]. Briefly, the scattering pattern was first divided into n parts equally along its equator direction from beam center, which was consistent to scattering vector ($s = 2\sin\theta/\lambda$) of s_1, s_2, s_3, …s_n. The intensity of the scattering pattern along azimuthal scan was then integrated at the scattering vector s_1, s_2, s_3, …s_n. All scattering patterns were fitted at low angle with the same region to increase reliability of relative comparison. The relationship between the integration breadth $B_{\pi/2}(s)$ and the scattering vector s was built as:

$$s^2 B_{\pi/2}^2(s) = \frac{1}{L^2} + s^2 B_{\text{eq}} \tag{4}$$

where $B_{\pi/2}(s)$ is the integration breadth along azimuthal scan, L is the length of the microvoids, and B_{eq} is the orientation angle of the microvoids. Fitting the experimental data using Eq. (4) can result the length of the microvoids L and the orientation angle of the microvoids B_{eq}. The experimental data and their fitting results are depicted in Fig. 1.

RESULTS AND DISCUSSION

The Raman spectra of the first-order region of carbon fibers heat treated at various temperatures are shown in Fig. 2(a). There are two main Raman modes observed in these spectra, one at about 1580 cm^{-1} assigned to the in-plane displacement of the carbons strongly coupled in the hexagonal sheets (G-line) and the other at

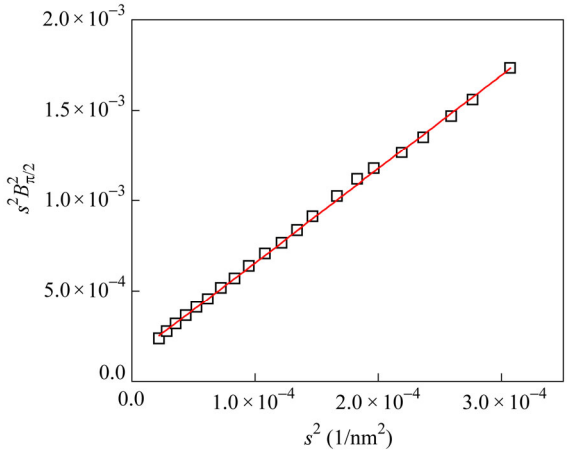

Fig. 1 $s^2 \sim s^2B_{\pi/2}^2$ plot of sample treated at 2400 °C

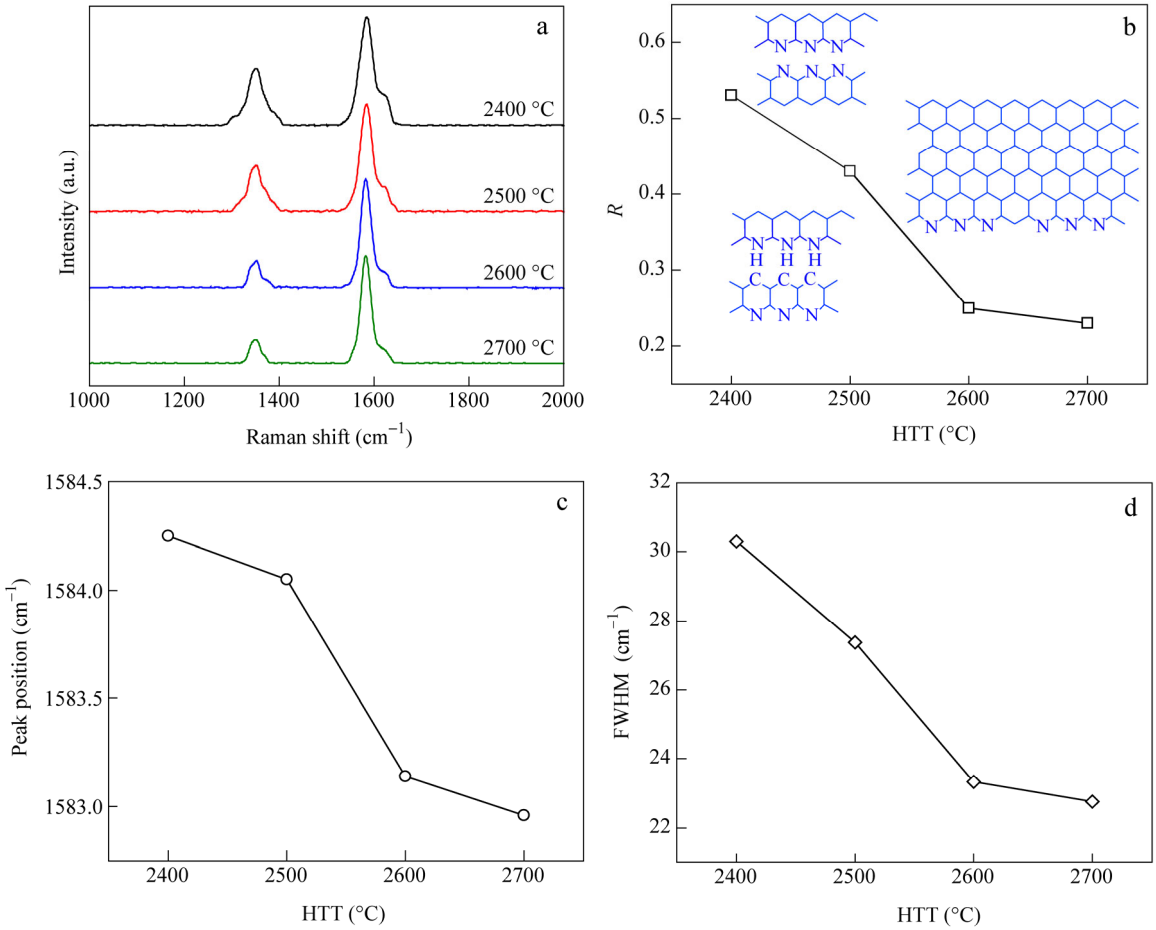

Fig. 2 Raman spectra of carbon fibers treated at different HTT (a); The ratio *R* (b), peak position (c) and FWHM (d) of G-line as a function of HTT

about 1360 cm^{-1} corresponded to the defect-induced Raman line (D-line). The shape of G-line becomes sharper and the intensity of D-line decreases with the increase in the treating temperature. Simultaneously, the content of

the ordered graphite structure increases. However, the D-line existed even after heat treated at 2700 °C, which indicated that there were still some disordered carbons in carbon fibers. The Raman spectroscopic parameters such as peak position, FWHM and *R* obtained after curve fitting are summarized in Table 1.

Table 1 Raman results of the carbon fibers obtained at different HTT

HTT (°C)	D-line			G-line			D′-line			*R*
	P (cm^{-1})	*W* (cm^{-1})	*I* (a.u.)	*P* (cm^{-1})	*W* (cm^{-1})	*I* (a.u.)	*P* (cm^{-1})	*W* (cm^{-1})	*I* (a.u.)	
2400	1350.44	37.04	0.55	1584.25	30.30	1.05	1622.89	15.83	0.17	0.52
2500	1350.06	33.67	0.45	1584.05	27.37	1.05	1622.68	15.53	0.13	0.43
2600	1349.75	24.76	0.26	1583.14	23.34	1.05	1622.45	11.85	0.08	0.25
2700	1349.61	23.33	0.24	1582.96	22.76	1.05	1621.92	11.82	0.06	0.23

P is peak position, *W* is FWHM, and *I* is peak intensity.

Figure 2(b) shows distinct differences in the ratios of the relative intensity of the Raman peaks *R* at different HTT. The ratio *R* decreases dramatically from 0.52 to 0.23 with increasing HTT, which illustrates the increase in the degree of graphitization of carbon fibers. Figures 2(c) and 2(d) display the peak positions and FWHM of the G-line at around 1580 cm^{-1} as a function of HTT, respectively. The results mean that the peak position of the G-line shifts to low wavenumbers (cm^{-1}) and approaches to 1582 cm^{-1} for the single crystal graphite. Meanwhile, the FWHM of the G-line peak becomes narrow with the increase in HTT, indicating a high degree of uniformity in the frequency of vibration in E_{2g2} in graphite lattice, which means the order in the hexagonal sheet is enhanced. The results indicate that defect structures originally presented in the carbon fibers are gradually healed during the higher temperature treatments. The increase in HTT is beneficial to improve the ordered three dimensional graphite crystalline structures in carbon fibers[5, 18].

XRD is a powerful method for characterizing the structures of various carbon materials. XRD curves by equatorial scan parallel and perpendicular to the axis of the carbon fibers at different HTT are shown in Figs. 3(a) and 3(b), respectively. In the XRD equatorial scan curves along the axis of the carbon fibers (Fig. 3a), two main peaks at about 26.4° and 54.2° can be observed, corresponding to (002) and (004) reflections of the pseudo-graphitic structure, respectively. The weak peak at about 42.7° arises from the (101) turbostratic plane of disordered carbon materials, which could only be identified as a very broad hump. The (002) peak profiles become sharper and more symmetrical with the increase in HTT, and its position slightly shifts to high angle. The results illustrate that the content of disorder structures, such as turbostratic layer structure, decreases during the process of HTT. Specifically, the higher the HTT is, the lower the content disorder structures in the carbon fibers will be. In the XRD curves by equatorial scan perpendicular to the carbon fiber axis (Fig. 3b), two main peaks at around 43.3° and 78.4° can be clearly identified, corresponding to the (100) and (110), respectively. These peaks become narrower with increasing HTT, which reveals that the in-plane structure of the graphite crystallites in the carbon fibers becomes more perfect with the increase of the HTT. Figures 3(c)–3(f) are the parameters which were calculated from the XRD curves. The changes of interlayer *d*-spacing d_{002} and crystal size parameters L_c and L_a of the graphite in the carbon fibers after heat treatment at different temperatures are summarized in Table 2. The interlayer space d_{002}, an indicative parameter of the degree of graphitization, decreases with the increase in HTT (Fig. 3e). The sample treated at 2700 °C has a d_{002} of 0.3363 nm, which is close to 0.3354 nm for hexagonal graphite. The crystal size parameters L_c increased from 3.19 nm to 4.28 nm while L_a from 10.9 nm to 13.6 nm (Fig. 3f). The data confirm that high temperature treatment of carbon fibers results in the growth of graphite crystals in the carbon fibers because of the establishment of long-range in-plane order and a partial development of the three dimensional graphite structure in the fibers[19].

Figure 4 shows the azimuthal scan of the crystal face (002) of graphite and the preferred orientation angle *Z* of the carbon fibers treated at different HTT. The orientation angle *Z* of graphite crystallite along the fiber axis is defined as the angle between the (002) plane of the graphite crystals and the fiber axis. From Fig. 4(b), we can

see that Z decreases with the increase in the HTT, which confirms that higher HTT is beneficial for the alignment of graphite crystals along the fiber axis. The parameters of XRD results are summarized in Table 2.

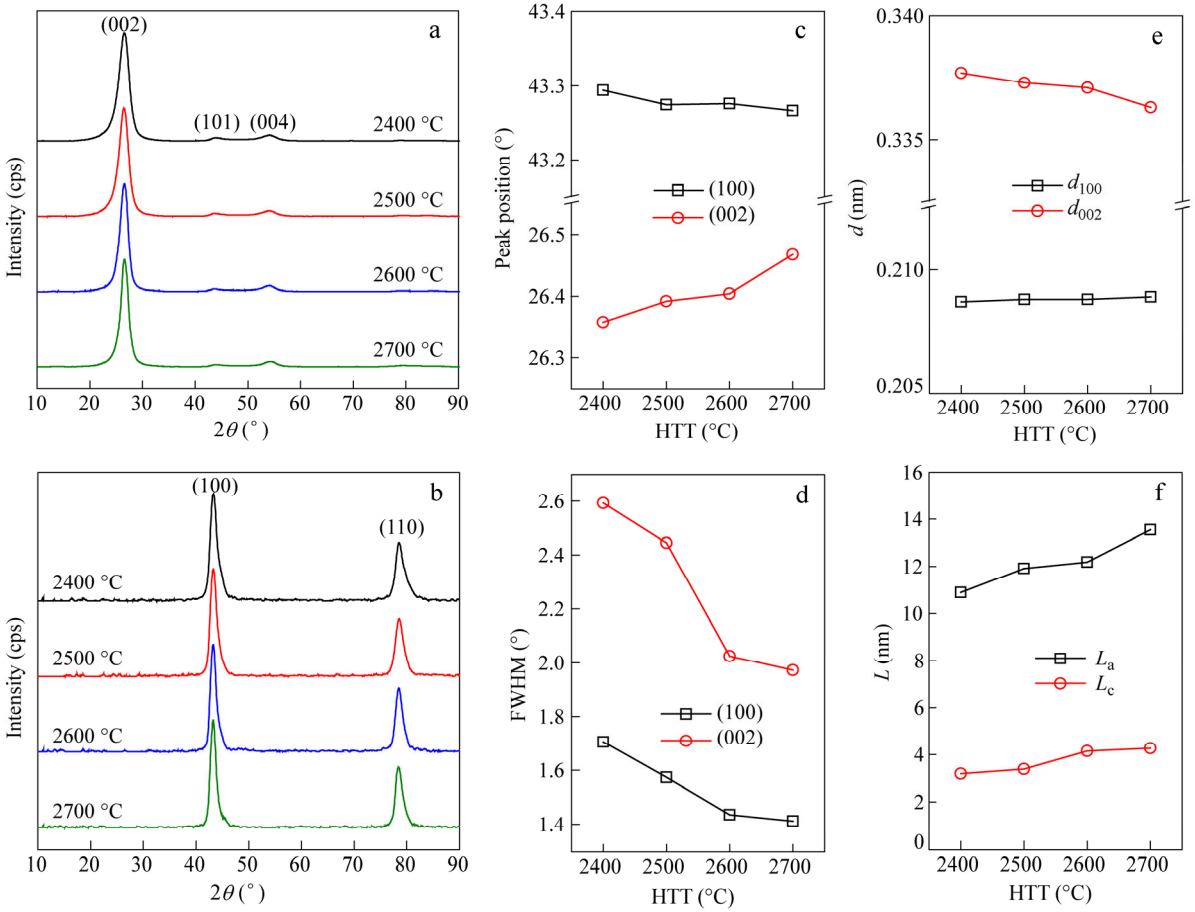

Fig. 3 XRD curves by equatorial scan (a) parallel and (b) perpendicular to the axis of the carbon fibers at different HTT; The peak position (c), FWHM (d), and d-spacing of (100) and (002), and the crystal size (f) as a function of HTT

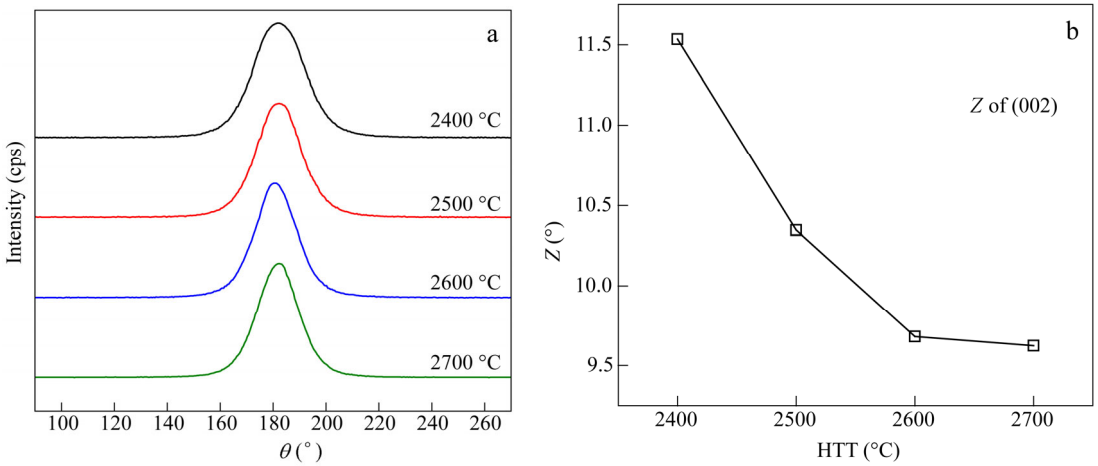

Fig. 4 (a) The XRD azimuthal scan curves in crystal face (002) of the carbon fibers treated at different HTT; (b) The preferred orientation angle of the graphite in the carbon fibers as a function of HTT

Table 2 XRD results of carbon fibers obtained at different HTT

HTT (°C)	(002)				(100)				*Z* (°)
	P (°)	*W* (°)	*d* (nm)	L_c (nm)	*P* (°)	*W* (°)	*d* (nm)	L_a (nm)	
2400	26.36	2.59	0.338	3.19	43.29	1.71	0.209	10.89	11.53
2500	26.39	2.45	0.337	3.39	43.27	1.57	0.209	11.91	10.35
2600	26.40	2.02	0.337	4.15	43.28	1.44	0.209	12.17	9.68
2700	26.47	1.97	0.336	4.28	43.27	1.41	0.209	13.55	9.62

Figure 5 presents the morphology of the graphite crystallites in carbon fibers treated at different HTT. The crystallite structure of carbon fibers is in the wavelike and winkled ribbons, corresponding to a turbostratic carbon structure, which is only ordered in two dimensions and less-ordered in three dimensions. In this turbostratic structure, graphite layer is twisted to each other through strong covalent bond force in plane and weak valence force between layers. The winkled ribbons transform to linear strip with the wavelength increased and amplitude decreased on account of solution of wrinkle at the HTT.

The value of L_c is only 3–5 nm after heat treatment at 2400 °C (Fig. 5a). However, L_c changes drastically to about 8 nm after heat treatment at 2700 °C (Fig. 5d). The results confirm the establishment of a three dimensional stacking order of graphite layers in the carbon fibers, which can be seen clearly in Figs. 5(c) and 5(d). The lattice fringe of carbon fibers treated at 2700 °C shows a very high degree of preferred orientation compared to that of the carbon fibers treated at 2400 and 2500 °C, which suggests that the crystallite structure in carbon fibers develops under the high temperature heat treatment.

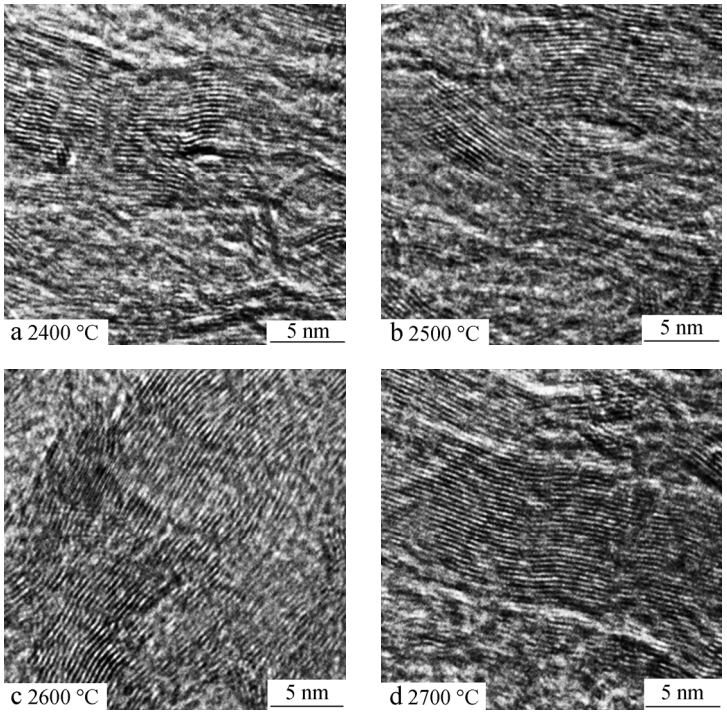

Fig. 5 HR-TEM images of lattice fringe images (002) of carbon fibers heat treated at various temperatures

During the high temperature graphitization treatment, rearrangement of carbon atoms in the carbon fibers takes place with the growth of graphite crystallites. In this process, the parameters of microvoids, which generally exist in carbon fibers, could be developed or changed at different HTT. The length *L* and the equatorial orientation distribution B_{eq} of microvoids were calculated from the SAXS experimental results according to the method in literatures[10, 11]. Figure 6 shows the length *L* and the equatorial orientation distribution B_{eq} of microvoids in the carbon fibers as a function of HTT. The length *L* of microvoids in the carbon fibers treated at

2400 °C is 85.72 nm, increasing with the raising HTT. In the case of carbon fiber treated at 2700 °C, L increases to 128.82 nm (Fig. 6a). Meanwhile, it can be seen that the equatorial orientation distribution B_{eq} of microvoids changed from 5.20° at 2400 °C to 7.00° at 2700 °C (Fig. 6b).

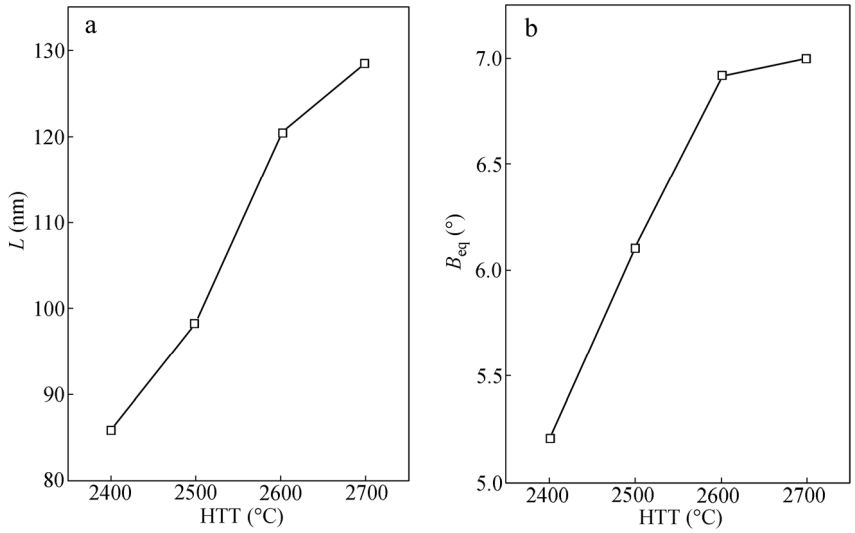

Fig. 6 (a) The length and (b) angle of orientation of microvoids

The rearrangement of carbon atoms and development of the defection in carbon fibers upon ultra-high temperature treatment can be depicted schematically in Fig. 7. As shown in Fig. 7, at elevated temperatures, the defection in graphite plane consisting of hexagonal network between graphite layers is reduced gradually owing to the rearrangement of carbon atoms. Meanwhile, pores of nanometer scale start to form and then contact with each other between the crystallites with the simultaneously reducing interlayer space and the increasing crystallite size of the graphite structure in the carbon fibers. Moreover, the size and equatorial orientation distribution of microvoids increase during the graphitization process. The formation of perfect and regular crystallite of graphite structure by graphitization process is necessary for preparation of high modulus carbon fibers. In addition, existence and development of microvoids are disadvantage for further improving the strength and modulus of carbon fibers. The present work will be helpful to set processing parameters for producing high strength and modulus carbon fibers.

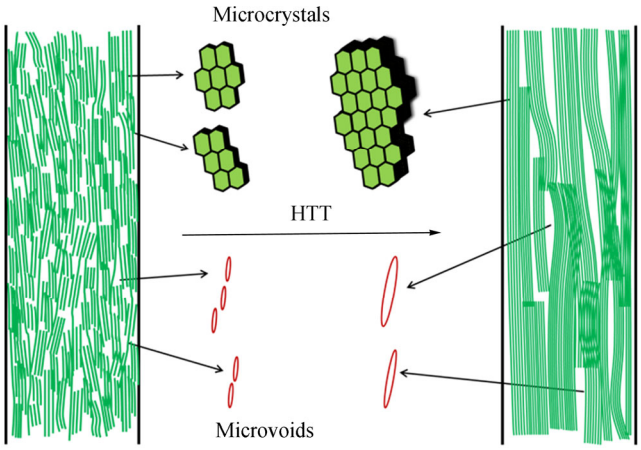

Fig. 7 Schematic diagrams for the three distribution morphologies of graphite crystallites

CONCLUSIONS

Microstructures of PAN-based carbon fibers during high temperature graphitization have been investigated by Raman, XRD, HR-TEM and SAXS. The crystalline size L_a and L_c increased distinctly with the increase of the treatment temperature, and the interlayer spacing d_{002} decreased simultaneously. Moreover, the preferred orientation of graphite crystallite along fiber axis decreased with the growth of crystalline size in fibers. In this process, the transformation of crystallite structure in carbon fibers occurred from wavelike graphite structure to three dimensional ordered graphite structure due to the rearrangement and compactness of graphite sheets. The microvoid structure of the fibers also changed in the high temperature graphitization stage. However, the reduction of nanoscale voids and growth of microscale voids are unfavorable for strength and modulus of carbon fibers based on the weakest link model. The large size and high degree of orientation of the graphite crystallites, as well as the small scale of voids conferred the properties of high modulus in the direction of the fibers. Therefore, reasonable control of the growth of graphite crystallites and the formation of microvoids is important for the preparation of high performance carbon fibers with both high strength and modulus.

REFERENCES

1 Rahaman, M.S.A., Ismail, A.F. and Mustafa, A., Polym. Degrad. Stab., 2007, 92(8): 1421
2 Edie, D.D., Carbon, 1998, 36(4): 345
3 Gao, A.J., Zhao, C., Luo, S., Tong, Y.J. and Xu, L.H., Mater. Lett., 2011, 65(23-24): 3444
4 Dobb, M.G., Guo, H., Johnson, D.J. and Park, C.R., Carbon, 1995, 33(11): 1553
5 Montes-Moran, M.A. and Young, R.J., Carbon, 2002, 40(6): 845
6 Montes-Moran, M.A. and Young, R.J., Carbon, 2002, 40(6): 857
7 Chaudhuri, S.N., Chaudhuri, R.A., Benner, R.E. and Penugonda, M.S., Compos. Struct., 2006, 76(4): 375
8 Zickler, G.A., Smarsly, B., Gierlinger, N., Peterlik, H. and Paris, O., Carbon, 2006, 44(15): 3239
9 Zhou, G.H., Liu, Y.Q., He, L.L., Guo, Q.G. and Ye, H.Q., Carbon, 2011, 49(9): 2883
10 Thunemann, A.F. and Ruland, W., Macromolecules, 2000, 33(5): 1848
11 Zhu, C.Z., Liu, X.F., Yu, X.L., Zhao, N., Liu, J.H. and Xu, J., Carbon, 2012, 50(1): 235
12 Fukuyama, K., Kasahara, Y., Kasahara, N., Oya, A. and Nishikawa, K., Carbon, 2001, 39(2): 287
13 Kaburagi, M., Bin, Y.Z., Zhu, D., Xu, C.Y. and Matsuo, M., Carbon, 2003, 41(5): 915
14 Zhu, C.Z., Yu, X.L., Liu, X.F., Mao, Y.Z., Liu, R.G., Zhao, N., Zhang, X.L. and Xu, J., Chinese J. Polym. Sci., 2013, 31(5): 823
15 Takaku, A. and Shioya, M., J. Mater. Sci., 1986, 21(12): 4443
16 Chieu, T.C., Dresselhaus, M.S. and Endo, M., Phys. Rev. B, 1982, 26(10): 5867
17 Tzeng, S.S., Carbon, 2006, 44(10): 1986
18 Tuinstra, F. and Koenig, J.L., J. Compos. Mater., 1970, 4(4): 492
19 Shim, H.S., Hurt, R.H. and Yang, N.Y.C., Carbon, 2000, 38(1): 29